HHS Public Access

Author manuscript

Andrology. Author manuscript; available in PMC 2024 July 01.

Published in final edited form as:

Andrology. 2023 July ; 11(5): 799–807. doi:10.1111/andr.13378.

Testis-specific proteins, TSNAXIP1 and 1700010I14RIK, are important for sperm motility and male fertility in mice

Yuki Kaneda[1,2], **Haruhiko Miyata**[1], **Keisuke Shimada**[1], **Seiya Oura**[1], **Masahito Ikawa**[1,2,3,4]

[1]Research Institute for Microbial Diseases, Osaka University, Suita, Osaka, Japan

[2]Graduate School of Pharmaceutical Sciences, Osaka University, Suita, Osaka, Japan

[3]The Institute of Medical Science, The University of Tokyo, Minato-ku, Tokyo, Japan

[4]Center for Infectious Disease Education and Research, Osaka University, Suita, Osaka, Japan

Abstract

Background: TSN (translin), also called testis brain RNA-binding protein, binds to TSNAX (translin-associated factor X) and is suggested to play diverse roles, such as RNA metabolism and DNA damage response. TSNAXIP1 (Translin-associated factor X-interacting protein 1) was identified as a TSNAX-interacting protein using a yeast two-hybrid system, but its function in vivo was unknown.

Objective: To reveal the function of TSNAXIP1 in vivo in mice.

Materials and methods: We generated *Tsnaxip1* knockout mice using the CRISPR/Cas9 system and analyzed their fertility and sperm motility. Further, we generated *1700010I14Rik* knockout mice, because 1700010I14RIK is also predominantly expressed in testes and contains the same Pfam (protein families) domain as TSNAXIP1.

Results: Reduced male fertility and impaired sperm motility with asymmetric flagellar waveforms were observed in not only *Tsnaxip1* but also *1700010I14Rik* knockout mice. Unlike *Tsn* knockout mice, no abnormalities were found in testicular sections of either *Tsnaxip1* or *1700010I14Rik* knockout mice. Furthermore, TSNAXIP1 was detected in the sperm tail and fractionated with axonemal proteins.

Discussion and conclusion: Unlike the TSN-TSNAX complex, whose disruption causes abnormal vacuoles in mouse testes, TSNAXIP1 and 1700010I14RIK may play roles in regulating sperm flagellar beating patterns.

Correspondence Haruhiko Miyata and Masahito Ikawa, Research Institute for Microbial Diseases, Osaka University, 3-1 Yamada-oka, Suita, Osaka 5650871, Japan. hmiya003@biken.osaka-u.ac.jp and ikawa@biken.osaka-u.ac.jp.

AUTHOR CONTRIBUTIONS

The study was designed by Yuki Kaneda, Haruhiko Miyata, and Masahito Ikawa. Data were collected by all authors, analyzed and interpreted by Yuki Kaneda, Haruhiko Miyata, and Masahito Ikawa. The manuscript was drafted by Yuki Kaneda and revised by Haruhiko Miyata and Masahito Ikawa. All authors read and approved the final version of the manuscript.

SUPPORTING INFORMATION

Additional supporting information can be found online in the Supporting Information section at the end of this article.

CONFLICT OF INTEREST

The authors declare they have no conflicts of interest.

Keywords

fertilization; knockout; sperm motility; testis; translin

1 | INTRODUCTION

Spermatogenesis is a specialized process by which spermatogonia differentiate into elongated spermatozoa by undergoing meiosis and subsequent spermiogenesis. During spermiogenesis, round spermatids undergo drastic morphological changes such as nuclear compaction and flagellar elongation, leading to the formation of spermatozoa. Spermatozoa are highly unique cells consisting of two distinct parts, heads and flagella. Sperm heads are composed of a nucleus and an acrosome, a specialized organelle containing enzymes that facilitate fertilization. Sperm flagella serve as a motility apparatus and can be divided into three parts, midpiece, principal piece, and end piece.[1,2] The midpiece possesses mitochondria that surround the axoneme, a 9+2 microtubular arrangement, and are thought to produce energy for sperm motility. The principal piece contains a rigid accessory structure called the fibrous sheath that serves not only as a structural component but also as a scaffold for several glycolytic enzymes that also produce energy for sperm motility. No accessory structures are found in the end piece, the tip of sperm flagella. Defects in sperm flagellar structures and/or functions often lead to impaired sperm motility and reduced fertility in men.

TSNAXIP1 (translin-associated factor X-interacting protein 1) was first identified as an interacting protein of TSNAX (translin-associated factor X) using yeast two-hybrid analysis.[3] TSNAX forms a heterodimer with TSN (translin) that is also called TB-RBP (testis brain RNA-binding protein).[4] The interaction between TSN and TSNAX was confirmed in male germ cells and brains.[5] The TSN-TSNAX complex is proposed to be involved in a variety of biological processes, such as regulation of RNA transport/translation/degradation and DNA damage response.[6,7] Knockout (KO) of *Tsn* in mice caused the loss of TSNAX in the testis and showed abnormal spermatogenesis, especially in aged (8-month old) mice with vacuoles observed in the seminiferous tubules, although *Tsn* KO mice did not exhibit impaired male fertility.[8] In the same study, no significant differences in sperm motility were found in *Tsn* KO mice compared to the control wild-type (WT) mice.[8] In contrast, functions of TSNAXIP1 in vivo are still unknown.

In this study, we disrupted TSNAXIP1 in mice using the CRISPR/Cas9 system and found that *Tsnaxip1* KO mice exhibited male subfertility. Further examination revealed that *Tsnaxip1* KO spermatozoa exhibited impaired motility. We also disrupted 1700010I14RIK, which has the same Pfam (protein families) domain as TSNAXIP1, and found that *1700010I14Rik* KO mice showed similar phenotypes to those of *Tsnaxip1* KO mice.

2 | MATERIALS AND METHODS

2.1 | Animals

All animal experiments performed in this study were approved by the Institutional Animal Care and Use Committees of Osaka University (Osaka, Japan) in compliance with the guidelines and regulations for animal experiments (approval code: H30–01-0; approval date: July 4, 2018). Mice were purchased from CLEA Japan, Inc. (Tokyo, Japan) or Japan SLC, Inc. (Shizuoka, Japan). WT or heterozygous mice were used for controls. Gene-modified mice generated in this study will be made available through either the RIKEN BioResource Research Center (ID number: RBRC11473 for *Tsnaxip1* KO mice; RBRC11494 for *1700010I14Rik* KO mice) or the Center for Animal Resources and Development (CARD), Kumamoto University (ID number: 3117 for *Tsnaxip1* KO mice; 3138 for *1700010I14Rik* KO mice).

2.2 | Pfam domain analysis of amino acid sequences

Amino acid sequences of TSNAXIP1 and 1700010I14RIK were obtained from the CCDS database (https://www.ncbi.nlm.nih.gov/projects/CCDS/CcdsBrowse.cgi). The sequence IDs of each amino acid sequence used were as follows: TSNAXIP1 (CCDS 22614.1) and 1700010I14RIK (CCDS28385.2). Pfam domain detection was performed using Simple Modular Architecture Research Tool (SMART) (http://smart.embl-heidelberg.de/).[9]

2.3 | Isolation of RNA and RT-PCR

RNA was isolated and purified from multiple adult tissues of C57BL/6N mice or testes from 1–5-week-old male mice using TRIzol (Thermo Fisher Scientific, MA, USA). Subsequently, reverse transcription was performed using the purified RNA and SuperScript IV Reverse Transcriptase (Thermo Fisher Scientific). The primers used for PCR of each gene are listed in Table S1.

2.4 | Generation of *Tsnaxip1* and *1700010I14Rik* KO mice using the CRISPR/Cas9 system

We designed gRNAs using CRISPRdirect software to reduce off-target possibilities.[10] Electroporation was performed as described previously.[11] Two gRNAs listed in Table S1 and tracrRNA (Merck, Darmstadt, Germany) were mixed with Cas9 protein (Thermo Fisher Scientific) and Opti-MEM (Thermo Fisher Scientific). This solution was incubated at 37°C to make the gRNA/Cas9 ribonucleoprotein complex, and the obtained complex was electroporated into fertilized oocytes (B6D2F1 X B6D2F1) using NEPA21 Super Electroporator (Nepagene, Chiba, Japan). The treated embryos reaching the two-cell stage were transplanted into the oviducts of ICR pseudo-pregnant females at 0.5 days after mating with vasectomized males. Pups were obtained by natural or caesarean section, and subsequent crosses with B6D2F1 WT mice or siblings were performed to obtain homozygous KO mice. Genotyping was performed using primers listed in Table S1. *Tsnaxip1* and *1700010I14Rik* double-KO mice were obtained by breeding of each KO mouse line.

2.5 | Fertility analysis of KO lines

Sexually mature B6D2F1 WT or KO male mice were housed individually with three 6-week-old female B6D2F1 mice for 3 months. The numbers of pups and copulation plugs were counted every weekday morning.

2.6 | Morphological and histological analysis of testis and epididymis

After euthanasia, testes and epididymides were dissected. After measuring the testicular weight, testes and cauda epididymides were fixed in Bouin's fluid (Polysciences, Inc., PA, USA), embedded in paraffin, sectioned, rehydrated, and treated with 1% periodic acid for 10 min, followed by treatment with Schiff's reagent (FUJIFILM Wako, Osaka, Japan) for 20 min. The sections were stained with Mayer's hematoxylin solution (FUJIFILM Wako) and observed using an Olympus BX53 microscope equipped with an Olympus DP74 color camera (Olympus, Tokyo, Japan).

2.7 | Analysis of sperm morphology and motility

Cauda epididymal spermatozoa were suspended in a drop of TYH medium.[12] For morphological analyses, spermatozoa were placed on MAS-coated glass slides (Matsunami Glass, Osaka, Japan) and observed using an Olympus BX53 microscope. Sperm motility was analyzed as described previously.[13] Spermatozoa obtained from the top of the TYH drop were analyzed using the CEROS II sperm analysis system (software version 1.5; Hamilton Thorne Biosciences, MA, USA) after 10 and 120 min of incubation. Spermatozoa were considered progressively motile when VSL/VAP ≥ 0.8 and VAP ≥ 50 μm/s. For sperm motility movies, waveform tracing, and maximum bending angles, spermatozoa were observed with an Olympus BX-53 microscope equipped with a high-speed camera (HAS-L1, Ditect, Tokyo, Japan). Waveforms of sperm flagellum were analyzed using the sperm motion analyzing software (BohBohsoft, Tokyo, Japan).[14] Maximum bending angles were measured using ImageJ (NIH, MD, USA).

2.8 | Immunoblot analysis

Testis and cauda spermatozoa were homogenized in lysis buffer containing 6 M urea, 2 M thiourea, and 2% sodium deoxycholate and incubate overnight at 4°C with rotation. The supernatant was collected after centrifuging at 15,000 × g for 15 min. Samples were subjected to SDS-PAGE under reducing condition using 5% 2-mercaptoethanol, followed by immunoblotting. After blocking with 10% skim milk in TBS containing 0.1% Tween-20, blots were incubated with primary antibodies at 4°C, and then incubated with secondary antibodies conjugated to horseradish peroxidase (1:5000, goat anti-mouse IgG [H+L] #115-036-062, goat anti-rat IgG [H+L] #112-035-167, or goat anti-rabbit IgG [H+L] #111-036-045, Jackson ImmunoResearch, West Grove, PA, USA) for 120 min at room temperature. Primary antibodies used: rabbit anti-TSNAXIP1 1:1000 (#17730-1-AP, Proteintech, IL, USA); rabbit anti-TSN antibody (a kind gift from Dr. Shin-ichi Kashiwabara, University of Tsukuba, Ibaraki, Japan)[15]; anti-SLC2A3 monoclonal antibody 1:1000, KS64-10[16]; anti-IZUMO1 monoclonal antibody 1:1000, KS64-125[17]; mouse anti-acetylated tubulin 1:5000 (#T7451, Sigma-Aldrich, MO, USA); rabbit anti-ODF2 1:1000 (#12058-1-AP, Proteintech); rat anti-PA tag 1:1000 (016-25861, FUJIFILM Wako); mouse

anti-FLAG tag (M2) 1:1000 (F1804, Sigma-Aldrich); and mouse anti-α-tubulin (B-5-1-2) 1:5000 (T5168, Sigma-Aldrich). Immunoreactive proteins were detected using Chemi-Lumi One Super (#02230, Nacalai Tesque, Kyoto, Japan) or Chemi-Lumi One Ultra (#11644, Nacalai Tesque).

2.9 | Separation of sperm heads and tails

Sperm head-tail separation was performed as previously described[18] with some minor modifications. Spermatozoa obtained from the cauda epididymis were suspended in 1 ml PBS and sonicated to separate tails from heads on ice (Sonifier SLPe, Branson Ultrasonics, CT, USA). The sample was centrifuged at 15,000 × *g* for 15 min. The pellet was then resuspended with 200 μl PBS and mixed with 1.8 ml of 90% Percoll solution (GE Healthcare, IL, USA) in PBS. After centrifugation at 15,000 × *g* for 15 min, sperm heads were at the bottom of the tube and the tails were in the top layer of the solution. The separated sample was diluted five-fold with PBS and centrifuged at 10,000 × *g* for 15 min. The pellets were washed twice with PBS and dissolved in lysis buffer containing 6 M urea, 2 M thiourea, and 2% sodium deoxycholate.

2.10 | Fractionation of spermatozoa protein

Fractionation of spermatozoa obtained from the cauda epididymis was performed as described previously[19,20] with some minor modifications. After sperm proteins were solubilized with 1% SDS lysis buffer (75 mM NaCl, 24 mM EDTA, pH 6.0), the samples were centrifuged at 15,000 × *g* for 10 min and the pellet was dissolved in lysis buffer containing 6 M urea, 2 M thiourea, and 2% sodium deoxycholate.

2.11 | Construction of expression plasmids

RNA obtained from C57BL/6N mouse testes was used to amplify cDNAs encoding *Tsnaxip1* and *1700010I14Rik*. *Tsnaxip1* cDNA and *1700010I14Rik* cDNA were cloned into a C-terminal FLAG-tagged pCAG vector[21] and a C-terminal PA-tagged pCAG vector, respectively. Primers used to construct the plasmid vectors are listed in Table S1.

2.12 | Cell culture and transfection

HEK293T cells[22] were cultured in DMEM (#11995–065, Thermo Fisher Scientific) supplemented with 10% fetal bovine serum (#S1560, Biowest, MO, USA) and 1% penicillin-streptomycin-glutamine (#10378–016, Thermo Fisher Scientific) at 37°C under 5% CO_2. The calcium phosphate transfection method was utilized to transiently transfect the plasmid DNA,[22] and cells were cultured for 24 h before harvesting.

2.13 | Immunoprecipitation

Transfected HEK293T cells were suspended in lysis buffer (1% Triton X-100, 20 mM Tris-HCl pH 7.4, 50 mM NaCl) containing protease inhibitor cocktail (#25955, Nacalai Tesque) and incubated for 1 h at 4°C. The lysates were centrifuged at 15,300 *g* for 5 min at 4°C. The obtained supernatants were incubated for 1 h at 4°C with anti-PA antibody-conjugated Dynabeads (#10009D, Thermo Fisher Scientific). After washing three times with wash buffer (40 mM Tris-HCl pH 7.5, 150 mM NaCl, 0.1% Triton X-100 and 10% glycerol), the

immune complexes were eluted with elution buffer (132 mM Tris HCl pH 7.4, 4% SDS, 20% glycerol, and 0.01% Bromophenol Blue). The eluents were subjected to SDS-PAGE for immunoblotting as described above.

2.14 | Ultrastructural analysis of sperm flagellum using TEM

Cauda epididymis was fixed with 4% PFA in PBS at 4°C. After the fixation, the samples were prepared as previously described,[23] and the ultrastructure was observed using a JEM-1400 plus electron microscope (JEOL, Tokyo, Japan) at 80 kV with a CCD Veleta 2K×2K camera (Olympus).

2.15 | Statistical analyses

Statistical analyses were performed using a two-tailed Welch's *t*-test by Microsoft Office Excel (Microsoft Corporation, WA, USA). *p*-Values lower than 0.05, 0.01, and 0.001 were considered significant (*), (**), and (***), respectively. Error bars in the graphs represent standard deviation.

3 | RESULTS

3.1 | TSNAXIP1 is important for male fertility

RT-PCR using RNA obtained from multiple mouse tissues showed that *Tsnaxip1* was specifically expressed in the testis while *Tsnax* was expressed ubiquitously in multiple tissues, with strong signals detected in the testis and ovary (Figure 1A), suggesting that *Tsnaxip1* may play specific roles in the testis. To determine which stage *Tsnaxip1* starts to express over the course of spermatogenesis, we performed RT-PCR using RNA obtained from mouse postnatal testes. Unlike *Tsnax, Tsnaxip1* started to express postnatally from 2 weeks when primary spermatocytes were seen (Figure 1B).[24] We then generated *Tsnaxip1* KO mice using the CRISPR/Cas9 system to examine the function of TSNAXIP1 in vivo. Two gRNAs were designed to largely delete the open reading frame (ORF) of *Tsnaxip1* (Figure 1C). Of the 58 fertilized oocytes that were electroporated, 40 two-cell embryos were transplanted into the oviducts of two pseudo-pregnant female mice, and 15 pups were born. Nine of the 15 pups had a large deletion, and subsequent crosses were performed to obtain homozygous KO mice. *Tsnaxip1* KO mice did not show any obvious abnormalities in development or behavior. Genotyping of obtained mice was performed by genomic PCR (Figure 1D) using the listed primers (Table S1), and subsequent Sanger sequencing revealed that obtained *Tsnaxip1* KO mice exhibited a 5,717 bp deletion (Figure 1E). We performed immunoblot analysis to confirm the depletion of TSNAXIP1 in *Tsnaxip1* KO testis and spermatozoa (Figure 1F). To examine if *Tsnaxip1* plays a role in male fertility, we caged individual *Tsnaxip1* KO males with three females for 3 months. Mating tests revealed that *Tsnaxip1* KO male mice exhibited impaired fertility compared to the WT control mice (Figure 1G), suggesting that *Tsnaxip1* is important for male fertility.

3.2 | *Tsnaxip1* KO mice showed reduced sperm motility with abnormal flagellar waveforms

To identify the cause of impaired male fertility found in *Tsnaxip1* KO mice, we initially examined spermatogenesis. No abnormalities were observed in testis gross morphology and

weights between the control and *Tsnaxip1* KO mice (Figure 2A,B). PAS staining of both testis and cauda epididymis showed no obvious differences between the two genotypes as well (Figure 2C and Figure S1A). Because it was reported that *Tsn* KO males showed increase in the number of vacuoles in seminiferous tubules as they got older,[8] we also observed testicular sections of aged *Tsnaxip1* KO mice (8-month old) (Figure S1B). However, no abnormalities were found even in aged *Tsnaxip1* KO testes, suggesting that the function of TSNAXIP1 may be different from that of TSN. Furthermore, when we obtained mature spermatozoa from the cauda epididymis, no obvious morphological defects were found in *Tsnaxip1* KO spermatozoa by phase contrast microscopy (Figure 2D).

We then assessed fertilizing ability of spermatozoa in vitro to elucidate the function of TSNAXIP1. In vitro fertilization (IVF) analysis using cumulus-intact oocytes revealed a significant reduction of fertilization rates in *Tsnaxip1* KO mice (Figure 3A) consistent with the result of mating tests (Figure 1G). However, the decrease in fertilization rates was rescued when the zona pellucida (ZP), an extracellular matrix surrounding the oocyte, was removed (Figure 3B). These results suggest that *Tsnaxip1* KO spermatozoa can undergo the acrosome reaction and fuse with eggs. We then performed computer-assisted sperm analysis (CASA) to evaluate sperm motility (Figure 3C). Although *Tsnaxip1* KO mice did not exhibit significant reduction in the percentage of motile spermatozoa compared to the control spermatozoa (Figure S2A), the percentage of progressively motile spermatozoa was significantly lower in *Tsnaxip1* KO mice than that of the control mice at 120-min incubation (Figure 3D), likely due to their circular motion (Figure 3C). Intriguingly, among velocity parameters such as VAP (average path velocity), VSL (straight-line velocity), and VCL (curvilinear velocity), there was a significant difference between the control and *Tsnaxip1* KO mice only in the VCL at 10-min incubation (Figure S2B), suggesting that impaired progressive motility is caused by the cumulative effect of changes in velocity parameters.

To further examine the defects in sperm motility, we traced the flagellar waveform (Figure 3E Movies S1 and S2). Flagellar beating pattern of control spermatozoa showed a symmetrical waveform, whereas *Tsnaxip1* KO spermatozoa showed an asymmetric waveform. This asymmetric waveform might result in circular motion and reduced progressive motility in *Tsnaxip1* KO mice (Figure 3C,D). In addition, we quantified maximum bending angles of the midpiece in primary anti-hook curvature after 120-min incubation in capacitating medium, which is used to quantitatively analyze hyperactivation.[25] In contrast to the control, *Tsnaxip1* KO spermatozoa exhibited low maximum bending angles, suggesting that *Tsnaxip1* is important for hyperactivation (Figure S2C).

3.3 | 1700010I14RIK contains the same TSNAXIP_N domain as TSNAXIP1 and its absence caused male subfertility with impaired sperm motility

Our laboratory has been analyzing testis-enriched genes by generating KO mice with the CRISPR/Cas9 system.[26,27] Among the testis-enriched genes, we found that 1700010I14RIK had the same Pfam domain called TSNAXIP_N as TSNAXIP1 by SMART analysis (Figure S3A), suggesting that 1700010I14RIK may have similar roles to that of TSNAXIP1. The TSNAXIP_N domains between TSNAXIP1 and 1700010I14RIK are 36% identical

at the amino acid sequence level.We confirmed that *1700010I14Rik* was predominantly expressed in the testis by performing RT-PCR using RNA obtained from multiple mouse tissues (Figure 4A). RT-PCR using RNA obtained from postnatal mouse testes revealed that *1700010I14Rik* started to express gradually postnatally from 2 weeks (Figure 4B) consistent with *Tsnaxip1* (Figure 1B). We then generated *1700010I14Rik* KO mice using the CRISPR/Cas9 system in the same way as *Tsnaxip1* KO mice to examine the function of 1700010I14RIK in vivo. Two gRNAs were designed to largely delete the ORF of *1700010I14Rik* (Figure 4C). Of the 145 fertilized oocytes that were electroporated, 120 two-cell embryos were transplanted into the oviducts of six pseudo-pregnant female mice and 28 pups were born. Fifteen of the 28 pups had a large deletion and subsequent crosses were performed to obtain homozygous KO mice. *1700010I14Rik* KO mice did not show any obvious abnormalities in development or behavior. We performed genomic PCR for genotyping (Figure 4D) using the listed primers (Table S1), and subsequent Sanger sequencing revealed that the *1700010I14Rik* KO mice have a 19,812 bp deletion (Figure 4E). To examine if *1700010I14Rik* plays a role in male fertility, we caged individual *1700010I14Rik* KO males with three females for 3 months. Mating tests revealed that *1700010I14Rik* KO mice exhibited impaired male fertility compared to the WT mice (Figure 4F), suggesting that *1700010I14Rik* is important for male fertility.

To identify the cause of impaired fertility found in *1700010I14Rik* KO males, we examined the testes; however, no abnormalities were found in testis gross morphology and weights between the control and *1700010I14Rik* KO mice (Figure S3B,C). PAS staining of both testis and epididymis showed no obvious differences between the two genotypes (Figure S3D). Furthermore, when we observed the morphology of spermatozoa obtained from the cauda epididymis by phase contrast microscopy, no obvious defects were found in *1700010I14Rik* KO spermatozoa (Figure S3E). We then performed CASA to evaluate sperm motility (Figure 4G). Although the percentage of motile spermatozoa in *1700010I14Rik* KO mice was comparable to that of the control mice (Figure S4A), the percentage of progressively motile spermatozoa was significantly lower in *1700010I14Rik* KO mice than that of the control mice at 120-min incubation (Figure 4H). Further analyses showed that velocity parameters such as VSL, VCL, and VAP at 120-min incubation were significantly impaired in *1700010I14Rik* KO mice compared to the control mice (Figure S4B). In addition, *1700010I14Rik* KO spermatozoa showed an asymmetric waveform (Figure 4I Movies S3 and S4) and low maximum bending angles (Figure S4C), which is similar to *Tsnaxip1* KO spermatozoa (Figure 3E and Figure S2C). These results suggest that the function of 1700010I14RIK may be similar to that of TSNAXIP1.

3.4 | *Tsnaxip1* and *1700010I14Rik* double-KO mice exhibit impaired male fertility but are not infertile

Because both TSNAXIP1 and 1700010I14RIK contain the same TSNAXIP1_N domain and each KO mice showed similar phenotypes, TSNAXIP1 and 1700010I14RIK may interact. Therefore, we co-expressed FLAG-tagged TSNAXIP1 and PA-tagged 1700010I14RIK in human embryonic kidney 293T (HEK293T) cells and performed an immunoprecipitation analysis using an anti-PA antibody. After immunoblot analysis, we found that TSNAXIP1 can interact with 1700010I14RIK (Figure S5A). We then examined the protein amounts of

TSNAXIP1 in *1700010I14Rik* KO males; however, there were no significant differences in the protein amounts of TSNAXIP1 between WT and *1700010I14Rik* KO testes and spermatozoa (Figure S5B), indicating that 1700010I14RIK depletion does not affect the amount of TSNAXIP1.

Because TSNAXIP1 exists in *1700010I14Rik* KO testis and spermatozoa, TSNAXIP1 may compensate the function of 1700010I14RIK. Therefore, we analyzed the phenotypes of *Tsnaxip1* and *1700010I14Rik* double-KO (dKO) males that were obtained by breeding of each KO mouse line. We caged individual dKO males with three females for 3 months and found that dKO males exhibited impaired fertility (Figure S6A), but were not infertile. This result indicates that male mice can still have some pups without both *Tsaxip1* and *1700010I14Rik*. Consistent with *Tsnaxip1* and *1700010I14Rik* single-KO males, dKO spermatozoa exhibited normal morphology (Figure S6B), but impaired motility with circular travel paths (Figure S7A-D). Further, consistent with *Tsnaxip1* and *1700010I14Rik* single-KO spermatozoa, dKO spermatozoa showed an asymmetric waveform (Figure S7E Movies S5 and S6) and low maximum bending angles (Figure S7F), but additional phenotypes not seen in either single KO were not found.

3.5 | TSNAXIP1 is localized in the sperm tail and fractionated with axonemal proteins

Because TSNAXIP1 was suggested to associate with TSN, we examined protein amounts of TSN in the testes and spermatozoa of *Tsnaxip1* KO, *1700010I14Rik* KO, and dKO mice. Immunoblot analysis revealed that KO of *Tsnaxip1, 1700010I14Rik*, or both genes did not affect protein amounts of TSN in the testes and spermatozoa (Figure 5A,B), while it was reported that the absence of TSN caused the loss of TSNAX in mouse testes.[8] These results support the idea that the function of TSNAXIP1 may be different from that of TSN.

We then analyzed the localization of TSNAXIP1 in the mature spermatozoa with immunofluorescence, but anti-TSNAXIP1 antibody did not work for immunofluorescence. Therefore, we sonicated mature spermatozoa to separate sperm heads and tails for immunoblotting and detected the TSNAXIP1 band in the tail fraction (Figure 5C). Further, we performed a sperm fractionation assay as described previously[19,20] and detected TSNAXIP1 in the Triton X-100 resistant/SDS-soluble fraction that contains axonemal proteins such as acetylated tubulin (Figure 5D). These results suggest that TSNAXIP1 may be localized in the axoneme and play roles in regulating the axoneme bending rather than RNA and DNA binding with TSN. Of note, no abnormalities were found in the ultrastructure of the axoneme with transmission electron microscopy even in *Tsnaxip1* and *1700010I14Rik* dKO spermatozoa (Figure 5E).

4 | DISCUSSION

In this study, we showed that *Tsnaxip1* and *1700010I14Rik* have the same Pfam domain called TSNAXIP1_N (Figure S3A), are predominantly expressed in the mouse testes (Figures 1A and 4A), and begin expression postnatally from 2 weeks (Figures 1B and 4B) when primary spermatocytes are first seen.[24] Further, we generated KO mice of each gene using the CRISPR/Cas9 system and found that each single-KO mouse line exhibited reduced male fertility due to impaired sperm motility. Both KO spermatozoa exhibit an asymmetric

waveform (Figures 3E and 4I), suggesting that both TSNAXIP1 and 1700010I14RIK may be involved in regulating flagellar bending patterns.

TSNAXIP1 was found to bind to TSNAX, an interacting protein of TSN that plays roles in RNA metabolism.[28] It was reported that aged *Tsn* KO mice (8-month old) as well as young *Tsn* KO mice (2-month old) showed abnormal vacuoles in testicular sections[8]; however, no abnormalities were found in the testicular sections of even aged *Tsnaxip1* KO mice (8-month old) (Figure S1B), suggesting that the interaction of TSNAXIP1 with the TSN-TSNAX complex is not critical for the function of TSN-TSNAX in spermatogenesis. Rather, TSNAXIP1 may play roles in regulating flagellar bending patterns as mentioned above. This idea is supported by the result that showed TSNAXIP1 localization in the sperm tail (Figure 5C). Further, TSNAXIP1 was found in the Triton X-100 resistant/SDS soluble fraction (Figure 5D), suggesting that TSNAXIP1 may be associated with the axoneme.

We also found that *1700010I14Rik* KO mice exhibited impaired sperm motility with abnormal flagellar waveforms, which is similar to *Tsnaxip1* KO mice. Using the heterologous expression system, we reveal that TSNAXIP1 can interact with 1700010I14RIK, although their relationship in vivo remains unknown. At least, our result showed that TSNAXIP1 was not depleted in the testes and spermatozoa of *1700010I14Rik* KO mice. Further, we found that *Tsnaxip1* and *1700010I14Rik* dKO male mice were subfertile, indicating that TSNAXIP1 and 1700010I14RIK are not essential for male fertility even if these genes work together. It remains to be determined if the common TSNAXIP_N domain is involved in the regulation of sperm motility.

In conclusion, we found two testis-specific genes, *Tsnaxip1* and *1700010I14Rik*, that are important for sperm motility and male fertility in mice. Amino acid sequences of both TSNAXIP1 and 1700010I14RIK are conserved well between mice and humans (Figure S8A,B). According to Genome Aggregation Database (gnomAD), a *TSNAXIP1* variant that causes a frameshift (p.Glu222ArgfsTer4) was found at high frequency (allele frequency: 0.001400) in humans, and two examples were found to possess the homozygous variant. Further analyses of *Tsnaxip1* and *1700010I14Rik* may lead to a better understanding of the etiology of human infertility.

Supplementary Material

Refer to Web version on PubMed Central for supplementary material.

ACKNOWLEDGMENTS

We thank Dr. Shin-ichi Kashiwabara and Dr. Yoshinori Kanemori (University of Tsukuba) for kindly providing rabbit anti-TSN antibody. We also would like to thank Ms. Eri Hosoyamada and Ms. Natsuki Furuta for technical assistance, and Dr. Julio M. Castaneda for critical reading of the manuscript.

Funding information

Ministry of Education, Culture, Sports, Science and Technology (MEXT)/Japan Society for the Promotion of Science (JSPS) KAKENHI, Grant/Award Numbers: JP21K19569, JP22H03214, JP20K16107, JP19H05750, JP21H04753, JP21H05033; Takeda Science Foundation; Japan Agency for Medical Research and Development (AMED), Grant/Award Number: JP21gm5010001; JST FOREST, Grant/Award Number: JPMJFR211F; Eunice Kennedy Shriver National Institute of Child Health and Human Development, Grant/Award Numbers:

P01HD087157, R01HD088412; Bill & Melinda Gates Foundation, Grand Challenges Explorations, Grant/Award Number: INV-001902

DATA AVAILABILITY STATEMENT

The data that support the findings of this study are available from the corresponding author upon reasonable request.

REFERENCES

1. Eddy EM, Toshimori K, O'Brien DA. Fibrous sheath of mammalian spermatozoa. Microsc Res Tech. 2003;61(1):103–115. doi:10.1002/jemt.10320 [PubMed: 12672126]
2. Miyata H, Morohoshi A, Ikawa M. Analysis of the sperm flagellar axoneme using gene-modified mice. Exp Anim. 2020;69(4):374–381. doi:10.1538/expanim.20-0064 [PubMed: 32554934]
3. Bray JD, Chennathukuzhi VM, Hecht NB. Identification and characterization of cDNAs encoding four novel proteins that interact with translin associated factor-X. Genomics. 2002;79(6):799–808. doi:10.1006/geno.2002.6779 [PubMed: 12036294]
4. Chennathukuzhi VM, Kurihara Y, Bray JD, Hecht NB. Trax (translin-associated factor X), a primarily cytoplasmic protein, inhibits the binding of TB-RBP (translin) to RNA. J Biol Chem. 2001;276(16):13256–13263. doi:10.1074/jbc.M009707200 [PubMed: 11278549]
5. Wu XQ, Lefrancois S, Morales CR, Hecht NB. Protein-protein interactions between the testis brain RNA-binding protein and the transitional endoplasmic reticulum ATPase, a cytoskeletal γ actin and trax in male germ cells and the brain. Biochemistry. 1999;38(35):11261–11270. doi:10.1021/bi990573s [PubMed: 10471275]
6. Wang J, Boja ES, Oubrahim H, Chock PB. Testis brain ribonucleic acid-binding protein/translin possesses both single-stranded and double-stranded ribonuclease activities. Biochemistry. 2004;43(42):13424–13431. doi:10.1021/bi048847l [PubMed: 15491149]
7. Li L, Gu W, Liang C, Liu Q, Mello CC, Liu Y. The translin-TRAX complex (C3PO) is a ribonuclease in tRNA processing. Nat Struct Mol Biol. 2012;19(8):824–830. doi:10.1038/nsmb.2337 [PubMed: 22773104]
8. Chennathukuzhi V, Stein JM, Abel T, et al. Mice deficient for testis-brain RNA-binding protein exhibit a coordinate loss of TRAX, reduced fertility, altered gene expression in the brain, and behavioral changes. Mol Cell Biol. 2003;23(18):6419–6434. doi:10.1128/mcb.23.18.6419-6434.2003 [PubMed: 12944470]
9. Letunic I, Khedkar S, Bork P. SMART: recent updates, new developments and status in 2020. Nucleic Acids Res. 2021;49(D1):D458–D460. doi:10.1093/nar/gkaa937 [PubMed: 33104802]
10. Naito Y, Hino K, Bono H,Ui-Tei K. CRISPRdirect: software for designing CRISPR/Cas guide RNA with reduced off-target sites. Bioinformatics. 2015;31(7):1120–1123. doi:10.1093/bioinformatics/btu743 [PubMed: 25414360]
11. Abbasi F, Miyata H, Shimada K, et al. RSPH6A is required for sperm flagellum formation and male fertility in mice. J Cell Sci. 2018;131(19):jcs221648. doi:10.1242/jcs.221648 [PubMed: 30185526]
12. Toyoda Y, Yokoyama M, Hosi T. Studies on the fertilization of mouse eggs in vitro. Jpn J Anim Reprod. 1971;16(4):147–151. doi:10.1262/jrd1955.16.152
13. Miyata H, Oura S, Morohoshi A, et al. SPATA33 localizes calcineurin to the mitochondria and regulates sperm motility in mice. Proc Natl Acad Sci U S A. 2021;118(35):e2106673118. doi:10.1073/pnas.2106673118 [PubMed: 34446558]
14. Baba SA, Mogami Y. An approach to digital image analysis of bending shapes of eukaryotic flagella and cilia. Cell Motil. 1985;5(6):475–489. doi:10.1002/cm.970050605
15. Oyama K, Baba T, Kashiwabara SI. Functional characterization of testis-brain RNA-binding protein, TB-RBP/translin, in translational regulation. J Reprod Dev. 2021;67(1):35–42. doi:10.1262/jrd.2020-120 [PubMed: 33268667]

16. Fujihara Y, Satouh Y, Inoue N, Isotani A, Ikawa M, Okabe M. SPACA1-deficient male mice are infertile with abnormally shaped sperm heads reminiscent of globozoospermia. Development (Cambridge). 2012;139(19):3583–3589. doi:10.1242/dev.081778

17. Ikawa M, Tokuhiro K, Yamaguchi R, et al. Calsperin is a testis-specific chaperone required for sperm fertility. J Biol Chem. 2011;286(7):5639–5646. doi:10.1074/jbc.M110.140152 [PubMed: 21131354]

18. Miyata H, Satouh Y, Mashiko D, et al. Sperm calcineurin inhibition prevents mouse fertility with implications for male contraceptive. Science. 2015;350(6259):442–445. doi:10.1126/science.aad0836 [PubMed: 26429887]

19. Cao W, Gerton GL, Moss SB. Proteomic profiling of accessory structures from the mouse sperm flagellum. Mol Cell Proteomics. 2006;5(5):801–810. doi:10.1074/mcp.M500322-MCP200 [PubMed: 16452089]

20. Castaneda JM, Hua R, Miyata H, et al. TCTE1 is a conserved component of the dynein regulatory complex and is required for motility and metabolism in mouse spermatozoa. Proc Natl Acad Sci U S A. 2017;114(27):E5370–E5378. doi:10.1073/pnas.1621279114 [PubMed: 28630322]

21. Niwa H, Yamamura KI, Miyazaki JI. Efficient selection for high-expression transfectants with a novel eukaryotic vector. Gene. 1991;108(2):193–199. [PubMed: 1660837]

22. Tiscornia G, Singer O, Verma IM. Production and purification of lentiviral vectors. Nat Protoc. 2006;1(1):241–245. doi:10.1038/nprot.2006.37 [PubMed: 17406239]

23. Shimada K, Kato H, Miyata H, Ikawa M. Glycerol kinase 2 is essential for proper arrangement of crescent-like mitochondria to form the mitochondrial sheath during mouse spermatogenesis. J Reprod Dev. 2019;65(2):155–162. doi:10.1262/jrd.2018-136 [PubMed: 30662012]

24. Kluin PM, Kramer MF, de Rooij DG. Spermatogenesis in the immature mouse proceeds faster than in the adult. Int J Androl. 1982;5(3):282–294. doi:10.1111/j.1365-2605.1982.tb00257.x [PubMed: 7118267]

25. Hwang JY, Mannowetz N, Zhang Y, et al. Dual sensing of physiologic pH and calcium by EFCAB9 regulates sperm motility. Cell. 2019;177(6):1480–1494.e19. doi:10.1016/j.cell.2019.03.047 [PubMed: 31056283]

26. Oyama Y, Miyata H, Shimada K, et al. CRISPR/Cas9-mediated genome editing reveals 12 testis-enriched genes dispensable for male fertility in mice. Asian J Androl. 2022;24(3):266–272. doi:10.4103/aja.aja_63_21 [PubMed: 34290169]

27. Miyata H, Castaneda JM, Fujihara Y, et al. Genome engineering uncovers 54 evolutionarily conserved and testis-enriched genes that are not required for male fertility in mice. Proc Natl Acad Sci U S A. 2016;113(28):7704–7710. doi:10.1073/pnas.1608458113 [PubMed: 27357688]

28. Gupta A, Pillai VS, Chittela RK. Translin: a multifunctional protein involved in nucleic acid metabolism. J Biosci. 2019;44(6):139. doi:10.1007/s12038-019-9947-6 [PubMed: 31894120]

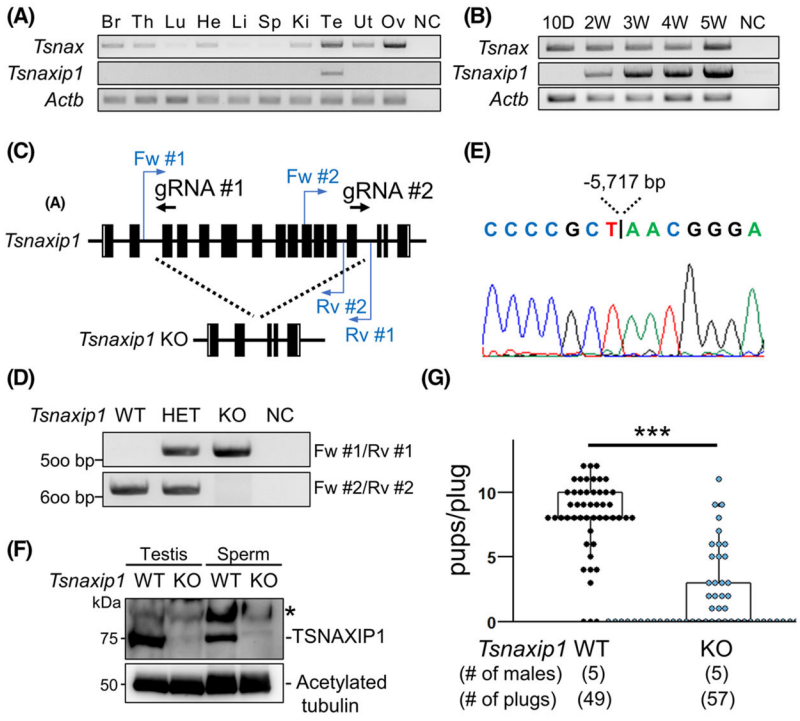

FIGURE 1.

TSNAXIP1 is important for male fertility. (A) Expression patterns of *Tsnaxip1* in mouse multiple tissues. *Actb* was used as a loading control. Br: brain, Th: thymus, Lu: lung, He: heart, Li: liver, Sp: spleen, Ki: kidney, Te: testis, Ut: uterus, Ov: ovary, and NC: negative control (water). (B) Expression of *Tsnaxip1* in testes at various postnatal days. *Actb* was used as a loading control. NC: negative control (water). (C) CRISPR/Cas9 targeting scheme of mouse *Tsnaxip1*. White boxes indicate untranslated regions while black shaded boxes indicate protein coding regions. Primers for genotyping are indicated in blue. (D) Genotyping of *Tsnaxip1* mutant mice. Fw #1-Rv #1 (for KO) and Fw #2-Rv #2 (for WT) primers in (C) were used. NC: negative control (water). (E) Wave pattern sequence of *Tsnaxip1* KO mice. *Tsnaxip1* KO allele exhibits a 5,717 bp deletion. (F) Confirmation of *Tsnaxip1* KO by immunoblotting. Acetylated tubulin was used as a loading control. Asterisk indicates nonspecific bands. (G) The number of pups born per plug detected. Three WT females were caged with each WT or *Tsnaxip1* KO male for 3 months. $p = 3.37 \times 10^{-19}$ (Welch's *t*-test).

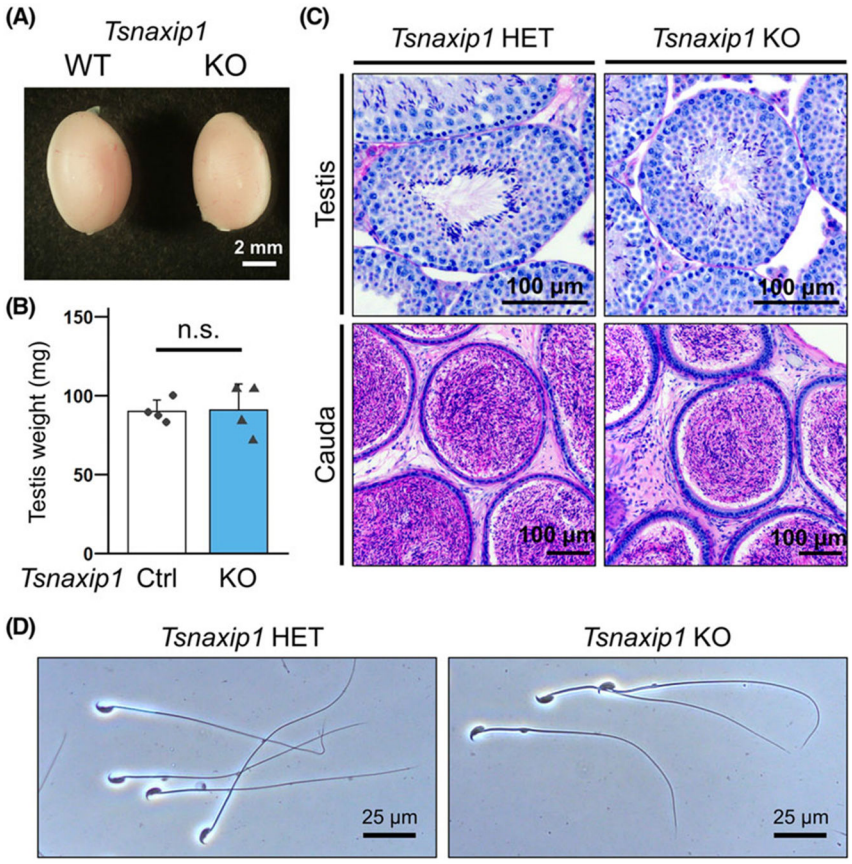

FIGURE 2.

Histological analyses and sperm morphology of *Tsnaxip1* KO mice. (A) Gross morphology of WT and *Tsnaxip1* KO testes. (B) Average weights of control and *Tsnaxip1* KO testes. $p = 0.916$ (Welch's *t*-test). (C) PAS staining of testis and cauda epididymis sections. (D) Observation of spermatozoa obtained from the cauda epididymis using phase contrast microscopy.

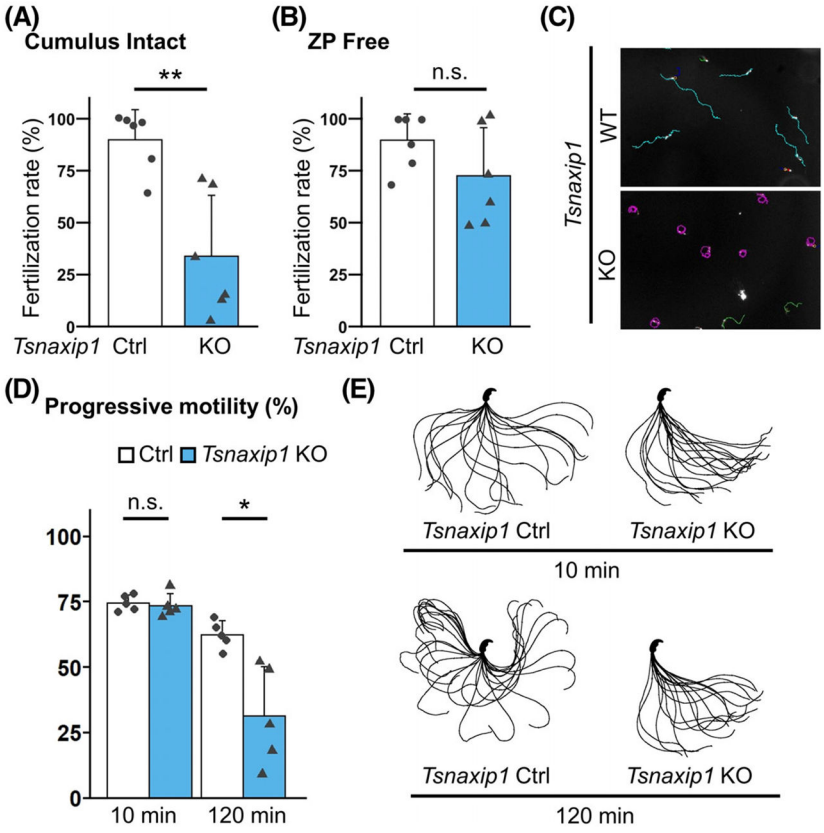

FIGURE 3.

TSNAXIP1 is important for sperm motility. (A) IVF analyses using cumulus-intact oocytes, $p = 0.0037$ (Welch's *t*-test). (B) IVF analyses using zona pellucida (ZP)-free oocytes, $p = 0.153$ (Welch's *t*-test). (C) Trajectories of moving spermatozoa analyzed by CASA (computer assisted sperm analysis) after 120-min incubation in TYH medium. Light blue tracks highlight progressively motile spermatozoa; green for motile; magenta for late (slow moving). Red points indicate immotile spermatozoa. (D) Percentages of progressively motile spermatozoa, $p = 0.737$ for 10 min and $p = 0.018$ for 120 min (Welch's *t*-test). (E) Sperm flagellar beating patterns were analyzed after 10- and 120-min incubation. Moving spermatozoa were videotaped at 200 frames per second, and one cycle of beating was indicated by superimposing videotaped images.

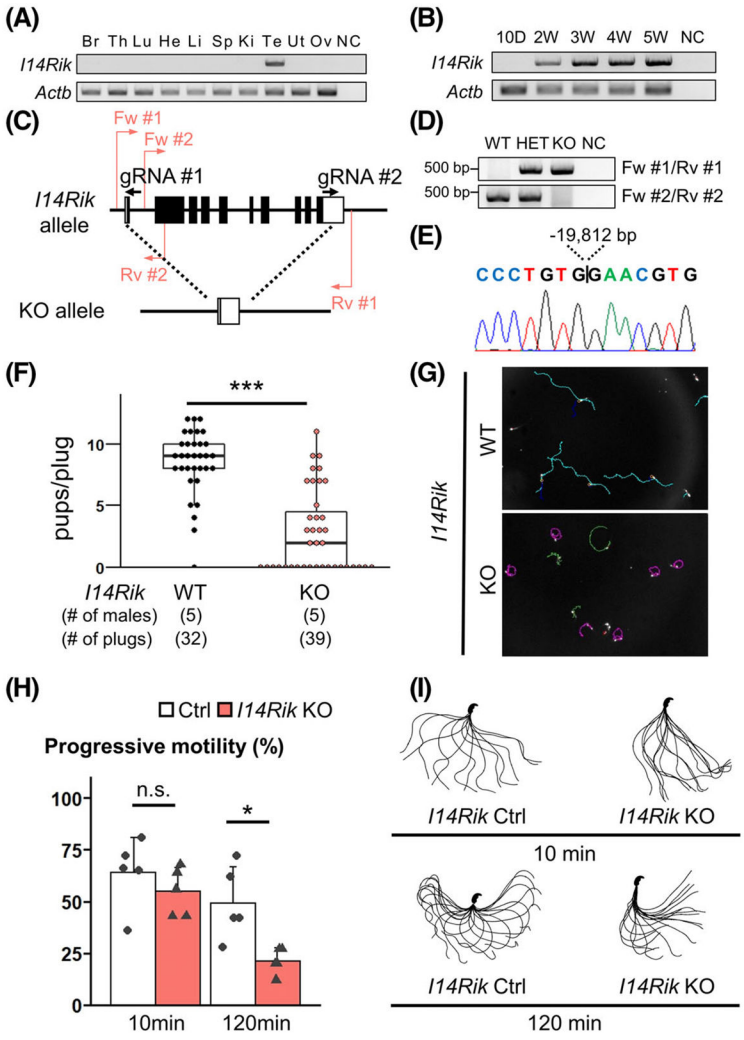

FIGURE 4.

1700010I14RIK is important for male fertility and sperm motility. (A) Expression patterns of *1700010I14Rik* in mouse multiple tissues. *Actb* was used as a loading control. Br: brain, Th: thymus, Lu: lung, He: heart, Li: liver, Sp: spleen, Ki: kidney, Te: testis, Ut: uterus, Ov: ovary, and NC: negative control (water). *1700010I14Rik* is shown as *I14Rik*. (B) Expression of *1700010I14Rik* in testes at various postnatal days. *Actb* was used as a loading control. NC: negative control (water). (C) CRISPR/Cas9 targeting scheme of mouse *1700010I14Rik*. White boxes indicate untranslated regions, while black shaded boxes indicate protein coding regions. Primers for genotyping are indicated in red. (D) Genotyping of *1700010I14Rik* mutant mice. Fw #1-Rv #1 (for KO) and Fw #2-Rv #2 (for WT) primers in (C) were used. NC: negative control (water). (E) Wave pattern sequence of *1700010I14Rik* KO mice. *1700010I14Rik* KO allele exhibits a 19,812 bp deletion. (F) The number of pups born per plug detected. Three WT females were caged with each WT or *1700010I14Rik* KO male for 3 months. $p = 1.59\times10^{-11}$ (Welch's *t*-test). (G) Trajectories of moving spermatozoa analyzed by CASA after 120-min incubation in TYH medium. Light blue tracks highlight progressively motile spermatozoa; green for motile; magenta for late (slow moving). Red points indicate immotile spermatozoa. (H) Sperm motility was analyzed 10 and 120 min

after incubation in TYH medium. Percentages of progressively motile spermatozoa are shown. $p = 0.349$ for 10 min and $p = 0.022$ for 120 min (Welch's *t*-test). (I) Sperm flagellar beating patterns were analyzed after 10- and 120-min incubation. Moving spermatozoa were videotaped at 200 frames per second and one cycle of beating was indicated by superimposing videotaped images.

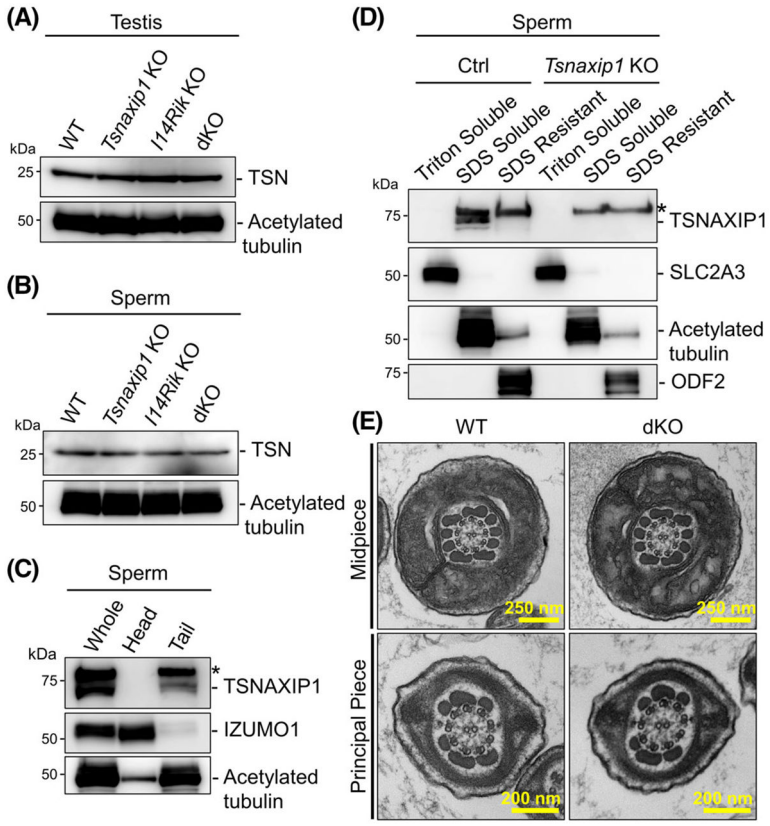

FIGURE 5.

TSNAXIP1 was detected in the sperm tail. (A) Immunoblot analysis of TSN in testes of WT, *Tsnaxip1* KO, *1700010I14Rik* KO, and dKO (*Tsnaxip1* and *1700010I14Rik*) mice. Acetylated tubulin was used as a loading control. *1700010I14Rik* is shown as *I14Rik*. (B) Immunoblot analysis of TSN in epididymal cauda spermatozoa of WT, *Tsnaxip1* KO, *1700010I14Rik* KO, and dKO mice. Acetylated tubulin was used as a loading control. (C) Head and tail separation of mouse spermatozoa. TSNAXIP1 was detected in the tail fraction. IZUMO1 and acetylated tubulin were detected as a marker for heads and tails, respectively. Asterisk indicates nonspecific bands. (D) Fractionation of sperm proteins using different lysis buffers. TSNAXIP1 was found in the SDS-soluble fraction that contains axonemal proteins. SLC2A3, acetylated tubulin, and ODF2 were detected as a marker for Triton-soluble, SDS-soluble, and SDS-resistant fractions, respectively. Asterisk indicates nonspecific bands. (E) Ultrastructure of sperm tails in *Tsnaxip1* and *1700010I14Rik* dKO mice. Cross-sections of midpiece and principal piece were observed using transmission electron microscopy.